Kinetics of Aging Process on Reduced Ag Exchanged Mordenite in Dry Air and Humid Air

Seungrag Choi[1,1], Yue Nan[1], and Lawrence Tavlarides[1]

[1]Syracuse University

September 11, 2020

Abstract

Aging effects of off-gas streams including dry air and humid air on reduced silver exchanged mordenite (Ag^0Z) were studied. Aged Ag^0Z was prepared by exposing Ag^0Z to dry air and humid air at different aging temperatures, time, and water vapor concentrations. Iodine loading capacity on the aged Ag^0Z was obtained through a continuous-flow adsorption system. Significant iodine loading capacity losses were observed after the Ag^0Z was exposed to dry air and humid air. Physical and chemical analyses were conducted to observe the physical and chemical changes of Ag^0Z after being aged. From iodine adsorption data and sample analyses, it was found that iodine loading capacity on the aged Ag^0Z in dry air and humid air decreases with increasing aging temperatures, time and water vapor concentrations. The pseudo reaction model describes experimental data well and the oxidation of Ag^0 is the rate determining step in the aging process.

Introduction

^{129}I is one of the volatile radioactive species in the off-gas stream generated from spent nuclear fuel reprocessing processes.^{129}I has a long half-life (1.6 x 10^7years) and it is fatal to the human body if released to the environment. Many studies have been carried out to capture radioactive iodine from spent nuclear fuel reprocessing off-gas streams. Liquid scrubbing methods have been reported[1, 2] for radioactive iodine removal, but these methods have a low removal efficiency, and require a high construction cost and additional works to reprocess toxic and acidic solutions produced from the liquid scrubbing processes. As an alternative to wet scrubbing systems, solid adsorbents to capture gaseous iodine have been also suggested.[1, 2] Of those studied solid adsorbents, hydrogen-reduced silver mordenite (Ag^0Z) has been introduced as a representative adsorbent which can effectively capture gaseous iodine. Various studies on Ag^0Z[3-9] have been reported including mechanisms and performances on iodine loading capacity.

In previous studies, many researchers investigated Ag^0Z reduced under a hydrogen environment, and discussed the reduction process, the mechanism, and the performance on the reduced silver mordenite.[3, 4]Ag^0 was formed on the surface of mordenite as larger particles through the reduction reaction in H_2, and it could capture gaseous iodine effectively in the form of crystalline AgI. These studies showed the formation of AgI on Ag^0Z exposed to gaseous iodine. To study the impact of off-gas streams on silver containing adsorbents, a number of aging studies have been performed. In efforts to understand the long-term behaviors of Ag^0Z in spent nuclear fuel reprocessing off-gas treatment, a number of aging studies on Ag^0Z[5-9] have been done for extended period of times up to 6 months. These studies showed the iodine loading capacities of Ag^0Z aged in gas streams at 150°C for up to 6 months decreased. For example, iodine loading capacity was decreased by 40% after exposure to dry air for 6 months[5] and by 60% after aging in humid air for 4 months.[6] Though the adverse effects of off-gas streams on Ag^0Z were investigated in previous studies, it is not clear why the iodine loading capacities of the adsorbents decreased when exposed to off-gas streams.

To understand the mechanisms of the aging processes on Ag^0Z, characterization studies including scanning

electron microscopy (SEM), X-ray photoelectron spectroscopy (XPS), and X-ray powder diffraction (XRD) were previously performed. It was found that Ag^0 was oxidized to Ag^+ by oxygen and water in dry air and humid air, then the oxidized Ag^+ was migrated into the pores of mordenite crystalline structure. Subsequently, Ag^+ was bound to the mordenite crystalline structure by replacing hydrogen detached from the mordenite. Finally, the replaced hydrogen was bound to oxygen or hydroxide to produce water.

The objective of this study is understanding aging processes of the selected adsorbent and to develop appropriate kinetic models to predict the effect of off-gas streams on silver containing adsorbents. To better understand the impact of off-gas streams including dry air and humid air on the silver containing adsorbent, Ag^0Z, the kinetics of the aging processes on Ag^0Z in off-gas streams were studied under experimental conditions including aging time (up to 6 months), temperatures (100 °C to 200°C), and water vapor concentrations (dew points: -40°C to +15 °C). The kinetic data from aging and iodine adsorption experiments were obtained, and a suitable reaction model was also recommended to predict the aging impacts on Ag^0Z.

Materials and Methods

Materials

The Ag^0Z used for this study was prepared by reducing the commercial AgZ (IONEX-Type, Ag-900 E16, Molecular Products) in a 4% H_2/Ar gas stream at 400 °C for 24 hours.[11] These reduction conditions were the optimal conditions to maximize iodine loading capacity on the Ag^0Z which were obtained from previous studies.[11, 13] Detailed physical properties of Ag^0Z were described previously[9]; the same material was used herein. Various gases used in this study, including compressed dry air (Ultra Zero Grade, dew point < -70 °C), N_2 (Ultra High Purity), and 4% H_2/Ar (Certified Standard Grade, 4% H_2 balanced in Ar), were purchased from Airgas Inc.

The Continuous-flow aging system

The aging experiments on the Ag^0Z in different types of gases for long times up to 6 months (10 minutes - 6 months) were performed to determine the impact of off-gas streams on the Ag^0Z. The experiments were done with the experimental system shown in Figure 1. The Ag^0Z was loaded into column sets, which are connected with stainless steel gas tubing in two ovens, and each column consisted of 5 sections. Each column was connected with gas-stream lines of dry-air and humid-air (d.p. -40°C, -15 °C, and +15°C), respectively. Thermocouples were placed at each stainless steel line in both ovens to monitor the gas temperature. The Ag^0Z loaded into column sets dried in a N_2 stream at 150 °C for 1 hour before starting the aging experiment to remove moisture and dust which may have existed in or on the Ag^0Z. Each gas was passed into each column through the gas lines for the designed periods at 150°C; flow rates were controlled by mass flow controllers at 500 ml/min. Water vapor was generated by a water vapor generator (Easidew, Michell Instruments) by controlling a dew point hygrometer which can be controlled by flow rates of the dry air stream. Each of the aged Ag^0Z samples were obtained after completion of aging at each desired aging time.

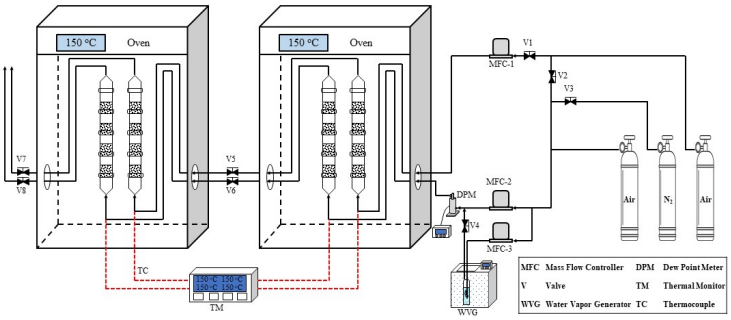

Figure 1. Schematic diagram of the continuous-flow aging system.

The Continuous-flow iodine adsorption system

Iodine adsorption experiments on the aged Ag^0Z were performed with the continuous-flow adsorption system shown in Figure 2 to quantify the impacts of off-gas streams on the iodine adsorption capacity of aged Ag^0Z. 50 ppmv of iodine vapors were generated from the dynacalibrators (VICI, model 450 and 500) by controlling flow rates of the carrier and dilution gas stream (dry air) at 500 ml/min. The aged Ag^0Z were loaded on a screen pan in a single layer inside adsorption column wrapped with glass coil, through which the flowing I_2 vapor was pre-heated at 150°C. The aged Ag^0Z samples were exposed to 50 ppm of gaseous iodine at 150 °C, and then the mass change of the aged Ag^0Z samples was measured by a microbalance connected with a screen pan inside adsorption column.

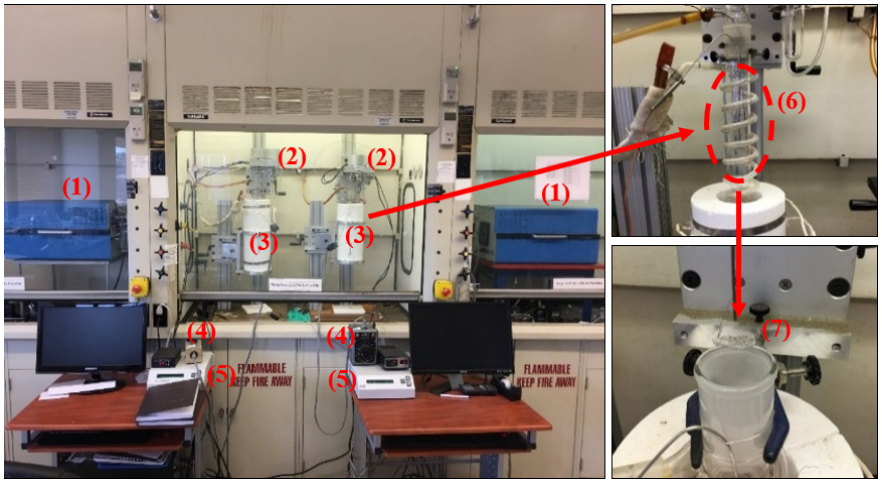

Figure 2. Photographs of the continuous-flow adsorption system; (1) Dynacalibrator; (2) Microbalance; (3) Furnace; (4) Temperature controller; (5) Data acquisition system; (6) Adsorption column; (7) Screen pan.

Characterization

Chemical analyses of each aged adsorbents were performed by various analytical techniques to determine the physical and chemical changes of Ag^0Z after being aged. Scanning Electron Microscopy (SEM, JEOL

5600) was employed to observe surface structure change on aged samples by obtaining information on each sample's surface and chemical composition.

X-ray diffraction (XRD, Bruker D8 Advance ECO powder diffractometer) equipped with a Cu Kα radiation (λ=1.540456 Å) at 40 kV and 25 mA was employed to observe the impacts of aging gases on $Ag^0$to describe behavior of silver particles. Diffraction patterns were collected at the 2ϑ-range between 15° and 60°, and the results were analyzed with the software MDI Jade version 9.0.

X-ray Photoelectron Spectroscopy (XPS, Surface Science Instruments SSX-100) in an ultrahigh vacuum was employed for surface elemental analysis to investigate the change of oxidation state of Ag in the adsorbents when exposed to the studied gas streams. A monochromatic Mg Kα X-ray source (1486.6 eV) at a working pressure in the analyzing chamber of ˜2 × 10-9 Torr was used to obtain the spectra. Survey/wide scans were performed using a pass energy of 150 V, and high-resolution scans were conducted with a pass energy of 50 V. A flood gun was used for charge neutralization. The binding energy (BE) of core-level Ag 3d was measured. C 1s peak at 284.2 ± 0.1 eV BE was taken as internal reference. Analysis of the data was performed with the Casa XPS program (Casa Software Ltd., UK).

Modeling

Pseudo kinetic model, which was first introduced by Lagergren[17] and widely used in various studies[18-22], was employed to express the deactivation of Ag as a function of aging time. The oxidation of Ag can be considered as a reversible reaction with an equilibrium in this study. The aging experiments in this study were conducted under a continuous flow system such that the concentrations of gas streams were constant during the aging processes. The pseudo reversible reaction model with a reaction equation (Eqn. 1) was applied to describe the kinetics of aging processes on Ag^0Z. C_{Ag} is the normalized concentration of silver which indicates the amount of I_2loaded on the aged Ag^0Z, A is a gas component used in this study, C_A is the concentration of oxygen in dry air,C_{Ag^+} is the concentration of silver oxidized by oxygen in dry air, n is the reaction order, k_1 is the forward reaction rate constant, and k_{-1} is the reverse reaction rate constant. Here k_1 and C_A are lumped into ${k_1}^*$because the gas concentration is constant all the time during aging experiment. The correlation coefficient (R^2) was also employed to determine the applicability of each model using Eqn. 2.x is sample data from experimental results, x is the average of the sample data set from experimental results, y is sample data from model results, and y is the average of the sample data set from model results. In general, as the correlation cofficient is close to 1, it indicates strong correlation between experimental data and model results.

$$\mathrm{AgAg_s}^{+}\backslash n \qquad v = \frac{\mathrm{dC_{Ag}}}{\mathrm{dt}} = -k_1 C_A {C_{\mathrm{Ag}}}^n + k_{-1} {C_{\mathrm{Ag^+}}}^n$$

$$k_1{}^* = k_1 C_A$$

$$v = \frac{\mathrm{dC_{Ag}}}{\mathrm{dt}} = -k_1{}^* C_{\mathrm{Ag}} + k_{-1} C_{\mathrm{Ag^+}}$$

$$\text{Correlation coefficient } \left(R^2\right) = \frac{\sum (x-x)(y-y)}{\sqrt{(x-x)^2 (y-y)^2}} \qquad (2)\backslash n$$

Results and Discussion

Aging effects of off-gas streams on the aged Ag^0Z

The data of iodine adsorption on the aged adsorbents are placed in Figure 3 which show iodine loading capacity on the Ag^0Z aged in dry air (d.p. < -70°C) and humid air (d.p. -15 °C) at 150 °C for up to 6

months (1 week ~ 6 months). Iodine loading capacity of the Ag^0Z decreases after being aged in dry air and humid air. The aged Ag^0Z samples in dry air for 1 week indicates that iodine loading capacity decreases to 10.5 wt.% from 12.3 wt.% (unaged Ag^0Z), and further decreases to 8.0 wt.% after being aged for 1 month. Iodine loading capacity of Ag^0Z aged in dry air for 1, 2, and 4 months shows similar drops which indicate no further degradation occurs during aging process over 1 month. A modest drop is observed after being aged for 6 months, but it could merely be owing to an experimental deviation caused by material nonuniformity. For the humid air aged Ag^0Z, iodine loading capacity decreases to roughly 6 wt.% which is dropping more rapidly than dry air. No further significant drops are observed after 1 month. Compared to the dry air aged Ag^0Z, these results suggest that the degradation rate increases as water is included in the air stream.

The decrease of maximum iodine loading capacity on both dry air aged and humid air aged Ag^0Z as a function of aging time are consistent with previous studies[5, 6] which show that dry air stream leads to a roughly 40% iodine capacity loss over 6 months and humid air stream leads to a roughly 50% iodine capacity loss over 6 months. However, the results of the aged Ag^0Z in humid air show less iodine capacity loss than previous studies[5, 6]. It is because a higher dew point of humid air (+15 °C) was used in previous studies than a dew point of humid air (d.p. -15 °C) used in this study. It is appropriate to expect that the lower concentration of water vapor used in this study would result in a less deactivation which is consistent with the following discussion on Figure 7. To summarize, in terms of iodine adsorption capacity loss on both dry air and humid air aged Ag^0Z, the aging effect of the humid air (d.p. -15°C) is higher than that of dry air.

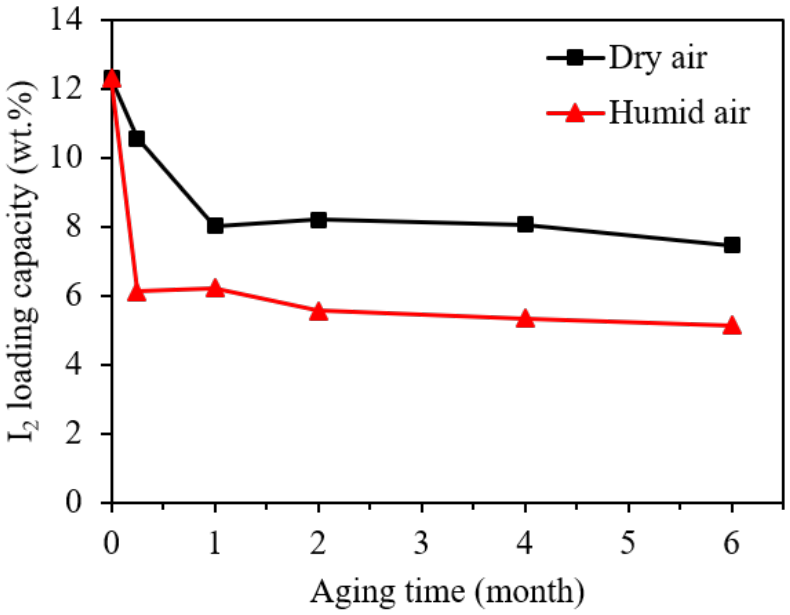

Figure 3. Iodine loading capacity on the aged Ag^0Z in dry air and humid air at 150 °C for up to 6 months.

Characterization

Scanning Electron Microscopy

SEM backscattered electron images for unaged AgZ, Ag^0Z, and aged Ag^0Z in dry air and humid air (d.p. -15 °C) for 1 month are shown in Figure 4. Small particles are observed on the mordenite crystal surface as shown in Figure 4b. White dots in the image indicates that they comprise elements of higher atomic mass than the Al, Si, and O that comprise the zeolite framework. According to the chemical composition of Ag^0Z,[11] these particles are necessarily composed of Ag atoms. This observation is in agreement with previous works

that indicate Ag ions (Ag^+) in AgZ are reduced to Ag^0 upon reduction in $H_2$with concomitant migration to the mordenite surface and formation of aggregate clusters.[14] This is also consistent with their absence in the image of AgZ (Figure 5a). The observed diameter of the Ag^0 particles ranged from 0.1 to 1.2 μm. While we expect particles smaller than 0.1 μm also exist, they cannot be observed under the current magnification. Although the I_2 loading capacity of Ag^0Z aged in dry air and humid air are decreased (Figure 3), a significant amount of Ag^0particles are observed on the surface of aged Ag^0Z in dry air (Figure 4c) and humid air (Figure 4d). It is because a reduction in amount or size of the Ag^0 particles cannot be quantitively observed by the SEM images.

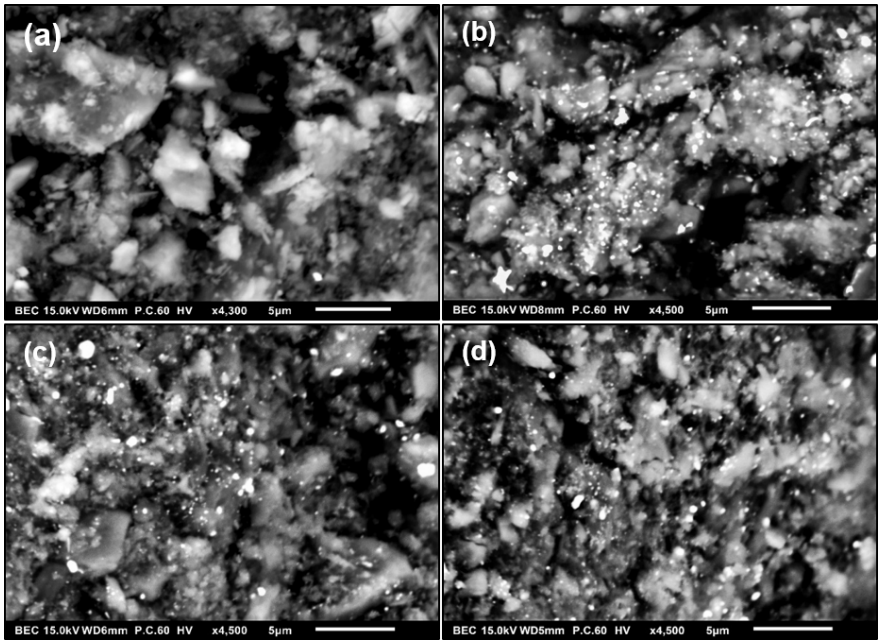

Figure 4. Scanning Electron Microscopy (SEM) images. (a) AgZ; (b) Ag^0Z; (c) Ag^0Z aged in dry air for 1 month; (d) Ag^0Z aged in humid air for 1 month.

X-ray Powder Diffraction

XRD patterns for the AgZ, Ag^0Z, and aged Ag^0Z in different gas streams including dry air and humid air are placed in Figure 5. The as-received AgZ exhibits a typical pattern at $10^\circ < 2\vartheta < 36^\circ$ for mordenite crystals. The patterns of Ag^0Z have two additional peaks at $2\vartheta = 38.2^\circ$ and $2\vartheta = 44.3^\circ$ corresponding to Ag crystals. This is in good agreement with the formation of Ag particles in Ag^0Z during the reduction in H_2. It also confirms that the particles observed in the backscattered electron images in Figure 4 are metallic Ag particles. Decreasing intensity of Ag crystal peaks is observed with all aged Ag^0Z in gas streams used in this study, indicating that the amount of Ag^0decreased during the aging process. This suggests that the Ag^0 was oxidized to other chemical forms when exposed to the gas streams. It is noted that the decrease in the quantity of Ag^0 in the aged Ag^0Z is consistent with the decrease in iodine adsorption capacity shown in Figure 3. This indicates that I_2 is adsorbed only by reaction with the Ag^0 particles and the oxidized $Ag^+$is not reactive or available to I_2. Furthermore, all aged Ag^0Z have the similar patterns for mordenite crystal as in Ag^0Z and AgZ, indicating that the crystal structure of mordenite is not affected by the aging process.

The XRD patterns also indicate that the aging gases have different oxidation effects on the Ag^0 particles in Ag^0Z. A portion of the silver in the Ag^0Z aged in dry air and humid air remained as Ag^0 which are consistent with the observations in the backscattered electron images shown in Figure 4. Besides, no additional characteristic peaks for crystals of Ag compounds (e.g. Ag_2O) are observed on the patterns of aged Ag^0Z, which

is also consistent with the observations in Figure 4. However, it is possible that Ag_2O exists as molecular species or small clusters, and thus are not detectable by the XRD.

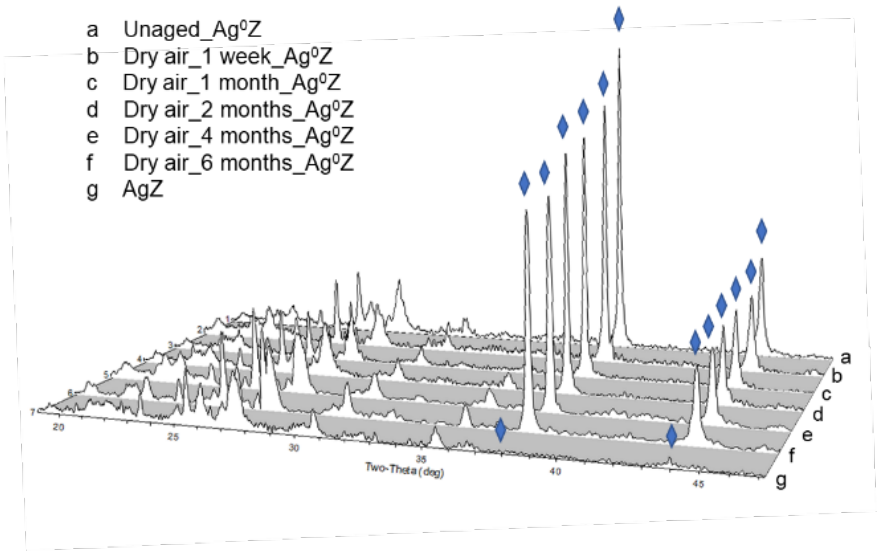

Figure 5. XRD patterns of AgZ, Ag^0Z, and aged Ag^0Z in dry air (top) and humid air (bottom) at 150°C.

X-ray Photoelectron Spectroscopy

XPS spectra for the AgZ, Ag^0Z, and aged Ag^0Z in dry air and humid air for 1 month and 2 months are shown in Figure 6. The results show that all samples have identical chemical compositions of Al, Si, and O, which when interpreted self-consistently with the aforementioned XRD results, confirm that the aging process does not impact on the chemical structure of mordenite crystals.

Ag 3d spectra for Ag standards and the Ag^0Z and the aged Ag^0Z samples are shown in Figure 6. The binding energy (BE) of Ag 3d5/2 measured for AgZ was 368.4 eV, and it shifted to 367.6 eV when the Ag^+ in AgZ was reduced and formed Ag^0 particles in Ag^0Z. It is noted that the Ag 3d5/2 BE for the Ag^0 particles in Ag^0Z is different to that for Ag foil standard (368.2 eV), which should be attributed to the chemical/physical environment of the Ag^0 particles as they locate in the macropores of the Ag^0Z.[4] These Ag 3d5/2 BEs are in agreement with those reported by Aspromonte and coworkers.[15] An increasing Ag 3d BE is noted when Ag^0Z was aged in aging gas streams used for this study. As highlighted in Figure 6, it shifts towards the Ag 3d BE for Ag_2O (368.3 eV) and AgZ (368.4 eV). Since no significant Ag_2O are detected by the XRD and XPS, this result suggests that the Ag^0Z was mainly oxidized back to AgZ when being aged in gas streams. Combining the results from SEM and XRD, it is most likely that the Ag particles are dispersed during the aging process. That is, the oxidized Ag^+ migrated back to the mordenite pores and channels, resulting in the same oxidation state as in AgZ. Since dry air and humid air are not as strong oxidants as NO_x, a portion of silver remained as Ag particles, and accordingly, the Ag 3d BEs for the aged samples in dry air and humid air are in between AgZ and Ag^0Z.

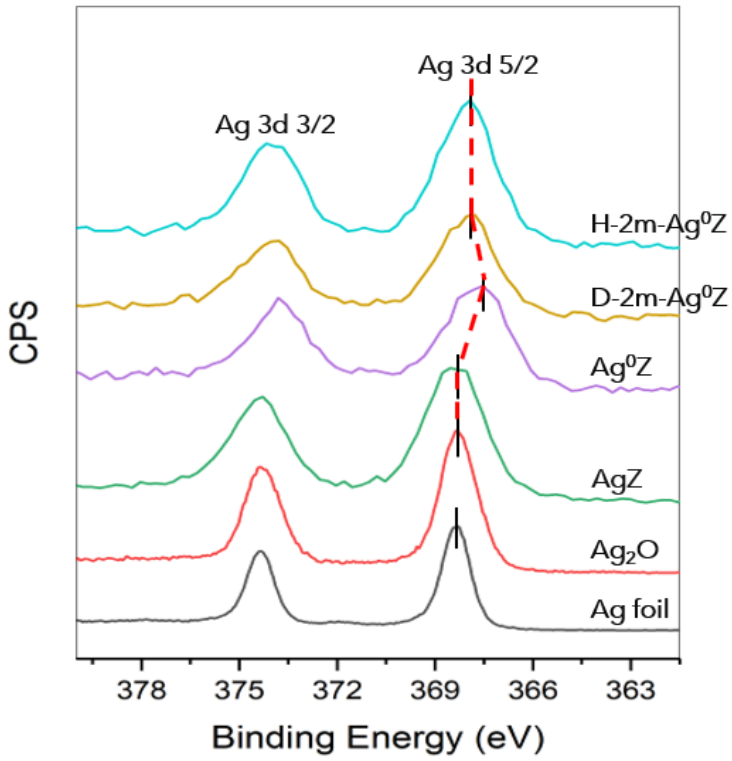

Figure 6. XPS spectra (Ag 3d core-level) of Ag standards, AgZ, Ag^0Z, and aged Ag^0Z in dry air and humid air at 150 °C for 2 months; D-2m-Ag^0Z is for the aged Ag^0Z in dry air for 2 months and H-2m-Ag^0Z is for the aged Ag^0Z in humid air for 2 months.

Kinetics of the aging process

Figure 3 shows the effects of dry air and humid air on the performance of Ag^0Z at 150 °C for up to 6 months. Especially, the aged Ag^0Z in dry air and humid air (d.p. -15 °C) showed a significant decrease of iodine loading capacities. For instance, the aged Ag^0Z in dry air and humid air for 1 month had a capacity loss for iodine by 34.7% and 49.4%, respectively. To obtain insight of the kinetics of aging on Ag^0Z, aging experiments under different conditions including time (1 day to 1 month), temperatures (100°C to 200 °C), and water vapor concentrations (d.p. -40 °C to +15°C) were performed.

Iodine loading data of each aged Ag^0Z sample was obtained and compared with the data of deactivation from the chemical analyses because the iodine capacity loss should be consistent with the amount of Ag which was oxidized. Figure 7 shows the kinetic data of iodine loading capacities on the Ag^0Z aged in different gas streams including dry air and humid air (d.p. -40°C, -15 °C, and +15°C) at different temperatures (100°C, 150 °C, and 200°C) for from 1 day to 1 month. The kinetic data shown in Figure 7 indicated that iodine loading capacities on the aged Ag^0Z decreased with increasing aging temperatures and time when exposed to off-gas streams, which mean that dry air and humid air have a negative impact on the iodine loading capacity of Ag^0Z. For example, iodine loading capacities on Ag^0Z aged in dry air (Figure (A)) decreased by 15.5%, 34.8%, and 36.4% at 100 °C, 150°C, and 200 °C after 1 month, respectively. Iodine loading capacities on Ag^0Z aged in humid air (d.p. -15 °C, Figure (B)) decreased by 42.4%, 44.8%, and 58.2% at 100 °C, 150°C, and 200 °C after 3 days, respectively. Figure (C) indicates the effect of water vapor concentration on iodine loading capacity of Ag^0Z; iodine loading capacities were decreased by 34.8% (d.p. -40°C), 44.8% (d.p. -15 °C), and 56.3% (d.p. +15 °C) at 150 °C after 3 days. Results in Figure 7 (B) and (C) show that the effect

of humid air increases with increasing temperatures and water vapor concentrations. The aging processes for short periods of time are sensitive to time, so some aging experiments were repeated to make sure of reliabilities of the results, and marked with standard error bars in Figure 7.

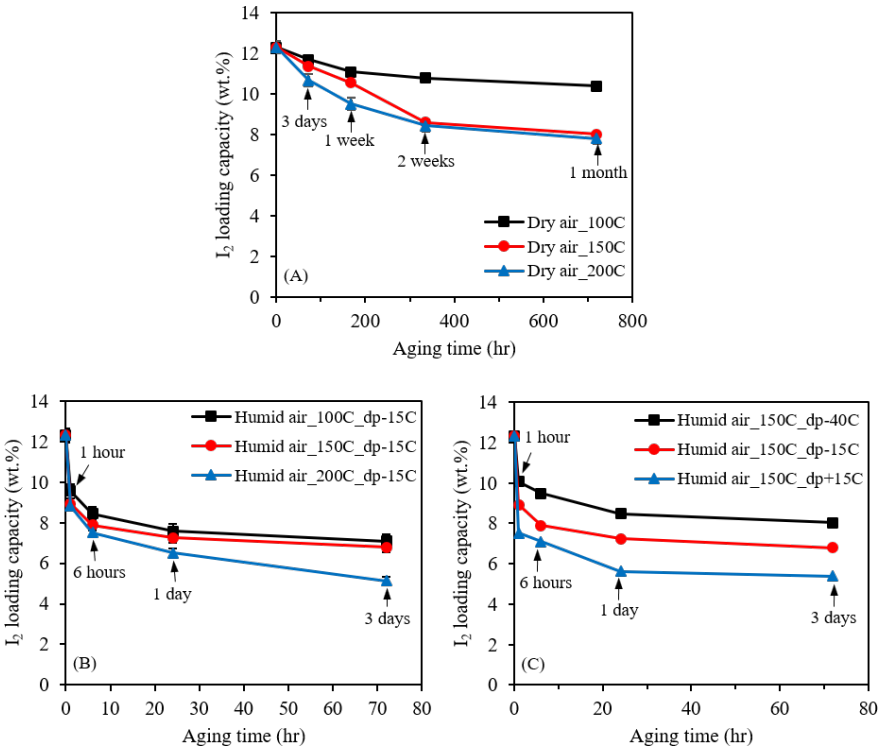

Figure 7. Kinetic data on Ag^0Z aged in dry air at different temperatures (A), humid air at different temperatures (B), humid air with different water vapor concentrations and constant temperature (C).

Aging mechanism

Based on experimental results and material characterizations, the aging processes on Ag^0Z occur through the Ag oxidation followed by the migration of Ag+ into the pores or channels of mordenite crystalline framework. Similar phenomena of Ag cluster dispersion in microporous zeolites including MFI[12] and Y zeolite[16] were also observed in previous studies. Thus, the pathways of the aging processes can be expressed as in the following steps; firstly, Ag^0 is oxidized to Ag^+ by oxygen which has existed in air gas streams, then the oxidized Ag^+ migrated into the pores of mordenite crystalline structure from the surface. After that, Ag^+ was bound to the mordenite crystalline structure through substitution with hydrogen. Finally, the generated hydrogen produced water by binding with oxygen or hydroxide.

In dry air as shown in Eqns. (3) ~ (6), Ag^0 is oxidized by O_2 in dry air to Ag^+ on the surface of the mordenite, then Ag^+ is migrated into the pores and bound to the crystalline structure in mordernite through subtitution reaction with H^+. The replaced H^+ was bound to the O^{2-} in order to produce H_2O. The different influences of the aging gas streams on Ag^0Z should depend on the different oxidation reactions of Ag^0Z. That is, the aging effects rely on the strength of the oxidants. The subsequent migration process, which is reactions (4) - (6) can be similar for the aging process in both gas streams. Considering the similar reactions (4) - (6) in both gas streams and the faster aging process in humid air (Figure 3) which shows higher iodine capacity loss after 1 week, it can be concluded that the aging processes in all gas streams used in this study are controlled by the oxidation reaction as shown in Eqns. (1) for dry air and (6) for humid air. The overall reaction, Eqn. (7), is proposed for the oxidation process of Ag cluster which is similar reaction as described

by previous study.[12]

$$O_2 + 4Ag 4\mathrm{Ag}_s{}^+ + 2O^{2-} \tag{3}$$

$$\mathrm{Ag}_s{}^+ \mathrm{Ag}_p{}^+ \tag{4}$$

$$\mathrm{Ag}_p{}^+ + HZ \; AgZ + H^+ \tag{5}$$

$$2H^+ + O^{2-} H_2O \tag{6}$$

$$Overall\ reaction: \quad O_2 + 4Ag + 4HZ 4AgZ + 2H_2O \tag{7}$$

Where Z representes mordenite, the subscript s denotes the Ag^+ on the external surface and p denotes the Ag^+ in the pores and channels of mordenite crystals.

In case of the aging process with humid air, an air stream containing water can promote the oxidation process based on experimental data and material analyses. The oxidation of Ag to Ag^+ with humid air takes place faster than with dry air by forming OH^- instead of O^{2-}. Then H_2O can be formed through a similar pathway in dry air as shown Eqns. (9) - (11). The overall reaction shown in Eqn. (12) is the same as that in dry air, but is catalyzed by water. Therefore, it can be expected that the effect of humid air on Ag^0Z will increases as the water vapor concentration increases.

$$2H_2O + O_2 + 4Ag 4\mathrm{Ag}_s{}^+ + 4OH^- \tag{8}$$

$$\mathrm{Ag}_s{}^+ \mathrm{Ag}_p{}^+ \tag{9}$$

$$\mathrm{Ag}_p{}^+ + HZ \; AgZ + H^+ \tag{10}$$

$$H^+ + \mathrm{HO}^- H_2O \tag{11}$$

$$Overall\ reaction: \; O_2 + 4Ag + 4HZ 4AgZ + 2H_2O \tag{12}$$

Modeling

As mentioned through the kinetic data and chemical analysis above, aging processes in dry air and humid air are controlled by the oxidation reaction. The aging experiments were conducted under a continuous flow system such that the concentrations of gas streams were constant during the aging processes. Accordingly,

the pseudo reversible reaction model was applied to describe the kinetics of aging processes on Ag^0Z. For the modeling work, the correlation coefficient (R^2) was used to evaluate the goodness of fit between experimental data and model results. According to the modeling results, pseudo 1st order reversible reaction models for aged Ag^0Z in dry air and humid air at different aging temperatures (100 °C, 150°C, and 200 °C) and different water vapor concentrations (d.p. -40 °C, -15°C, and +15 °C) for up to 2 weeks are placed in Figure 8 which are incorporated with the kinetic data shown in Figure 7.

Modeling results on the aged Ag^0Z in dry air at different temperatures for different aging time are shown in Figure 8 (A). Eqn. (13) represents a reaction equation for a kinetic model on the aged Ag^0Z in dry air shown in Figure 8 (A).C_{Ag} is the normalized concentration of silver which indicates the amount of I_2 loaded on the aged Ag^0Z, C_{O_2} is the concentration of oxygen in dry air, C_{Ag^+} is the concentration of silver oxidized by oxygen in dry air, n is the reaction order, and k_1 is the forward reaction rate constant, and k_{-1} is the reverse reaction rate constant. Here, k_1 and C_{O_2} are lumped into${k_1}^*$ because the gas concentration was constant all the time during the aging experiment. C_{Ag^+} can be calculated by substracting the amount of I_2 loaded on the aged Ag^0Z from the amount of I_2 loaded on the unaged Ag^0Z. The model parameters of all reaction models and correlation coefficients (R^2) between experimental data and model results are shown in Table 1. These results indicate a model is fitted to experimental data well when $n \geq 1$with strong correlation coefficient (for example, R^2 = 0.988 at 150 °C) using Eqn. 2, which means the Pseudo 1st reversible reaction model fits experimental data (Figure 8 (A)). These results are consistent with experimental data (Figure 7) that the aging effects of gas streams on Ag^0Z increase with increasing aging time and temperatures.

$$\mathrm{AgAg_s}^+ \qquad (13)\backslash nv$$

$${k_1}^* = k_1 C_{O_2}$$

$$v = \frac{\mathrm{dC_{Ag}}}{\mathrm{dt}} = -{k_1}^* C_{\mathrm{Ag}} + k_{-1} C_{\mathrm{Ag^+}} \quad (for\ n = 1)$$

Modeling results on the aged Ag^0Z in humid air with different temperatures, aging time, and water vapor concentrations are placed in Figure 8 (B) and (C). A reaction equation for the model is provided in Eqn. (14). Considering the results of correlation coefficient to each order model with the model results, when$n \geq 1$, model results show good fitting to experimental data.C_{H_2O} and C_{O_2} are the concentrations of water vapor and oxygen in humid air, k_1 is the reaction rate constant,k_{-1} is the reverse reaction rate constant, and n is the reaction order. Here, k_1, C_{H_2O}, and C_{O_2} are lumped into ${k_1}^*$, and m is the power of the water vapor concentration determined by a exponential curve expressed by${k_1}^*$ versus C_{H_2O} as shown in Figure 9 (m = 0.20). These modeling results indicate that the pseudo 1streversible reaction model fits experimental data (For example, R^2 = 0.985 at 150 °C) with similar approach to the model result of dry air aged Ag^0Z.

$$\mathrm{AgAg_s}^+ \qquad (14)$$

$$v = \frac{\mathrm{dC_{Ag}}}{\mathrm{dt}} = -{k_1}^* {C_{\mathrm{Ag}}}^n + k_{-1} {C_{\mathrm{Ag^+}}}^n$$

$${k_1}^* = k_1 {C_{H_2O}}^m C_{O_2}$$

$$v = \frac{\mathrm{dC_{Ag}}}{\mathrm{dt}} = -{k_1}^* C_{\mathrm{Ag}} + k_{-1} C_{\mathrm{Ag^+}} \quad (for\ n = 1)$$

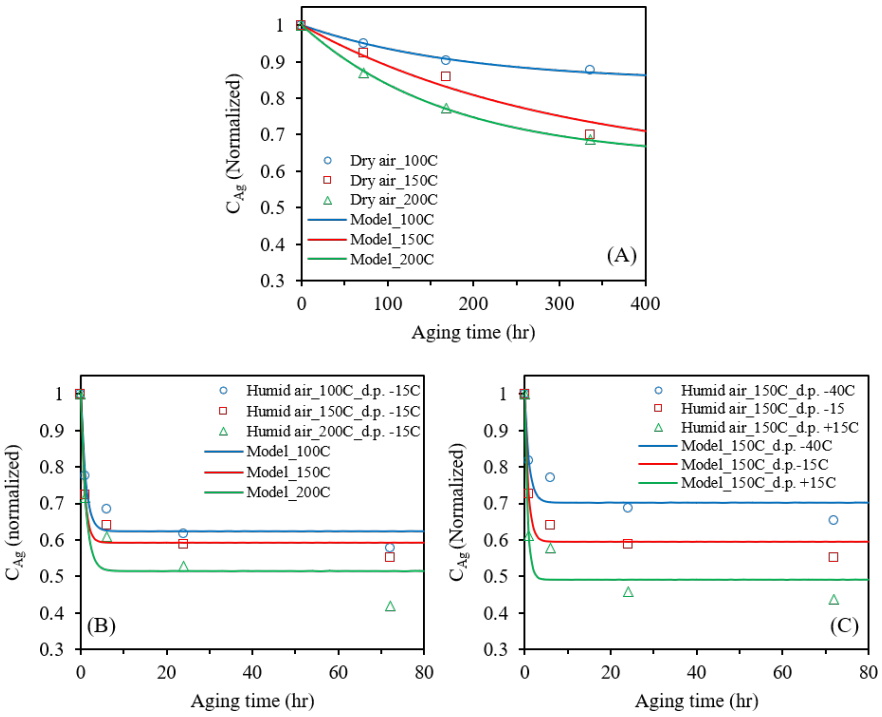

Figure 8. Pseudo 1st order reaction models on Ag^0Z aged in dry air (A), humid air (B), and humid air with different water vapor concentrations (C) at different aging temperatures and time.

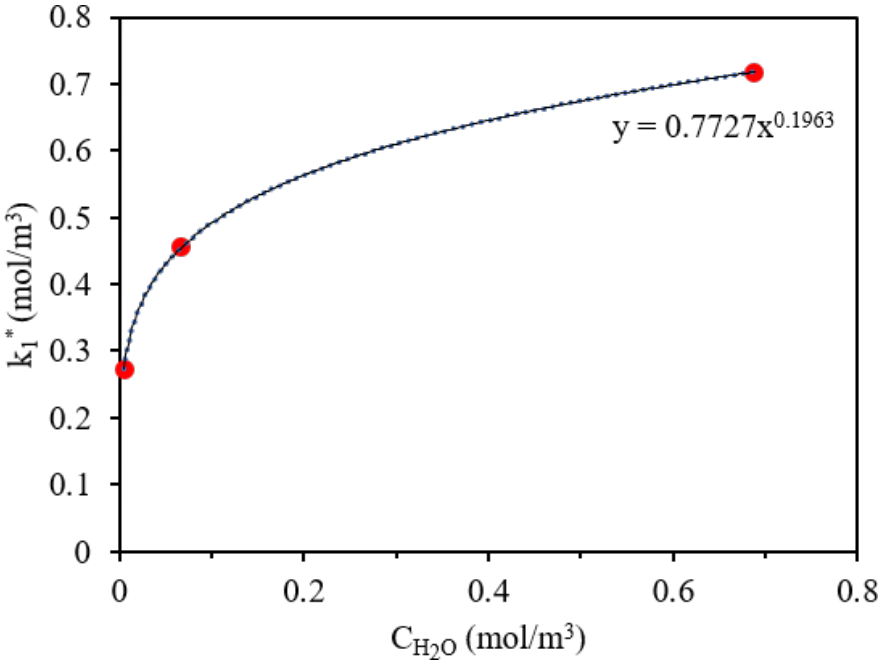

Figure 9. Power function curve between reaction rate constant ($k_1{}^*$) and water vapor concentration (C_{H_2O}).

Table 1. Variables and Model Parameters for the Pseudo Reaction Model

T (°C)	D.P. (°C)	C_{H2O} (mol/m^3)	C_{O2} (mol/m^3)	k_1* (hr^{-1})	k_1 ((mol/m^3)$^{-1}$·hr^{-1})	k_1 ((mol/m^3)$^{-1}$·hr^{-1})[a]	k_{-1}[a](hr^{-1})	$R^{2,b}$
Dry air								
100	-70	-	8.59	8.36E-4	8.36E-4	9.73E-5	4.55E-3	0.997
150	-70	-	8.59	1.32E-3	1.32E-3	1.53E-4	2.01E-3	0.988
200	-70	-	8.59	2.14E-3	2.14E-3	2.4E-4	3.68E-3	0.999
Humid air								
100	-15	0.067	8.59	0.323	0.323	0.064[a]	0.537	0.974
150	-40	0.005	8.59	0.272	0.272	0.090[a]	0.644	0.982
150	-15	0.067	8.59	0.456	0.456	0.090[a]	0.667	0.985
150	+15	0.687	8.59	0.716	0.716	0.090[a]	0.688	0.982
200	-15	0.067	8.59	0.403	0.403	0.080[a]	0.429	0.953

[a](mol/m^3)$^{-1.20}$·hr^{-1}for humid air

[b]for n = 1 in Eqns. (13) and (14).

Conclusion

The aging processes on Ag^0Z in dry air and humid air as off-gas streams from the spent nuclear fuel reprocessing system were studied. Iodine loading capacity of Ag^0Z after being aged in gas streams including dry air and humid air (d.p. -40°C, -15 °C, and +15°C) at 100 °C, 150°C, and 200 °C for up to 6 months were obtained. Iodine loading capacity of Ag^0Z aged in dry air and humid air (d.p. -15 °C) at 150°C for 1 month decreased by roughly 35% and 50%, respectively, which indicate that humid air has more adverse impact on the performance of the Ag^0Z. Besides, aging temperatures and water vapor concentrations are key factors which have negative influences on the Ag^0Z; iodine loading capacity was decreased with increasing aging temperatures and water vapor concentrations.

The aging mechanisms of Ag^0Z in dry air and humid air were suggested with SEM, XRD, and XPS analyses. It was found that the mechanism includes the following steps; (1) oxidation of Ag^0 to Ag^+, (2) migration of Ag^+ from the surface to the pores/channels of mordenite crystals, (3) binding of Ag^+ within the zeolite framework by replacing the H, and (4) binding of the generated H^+ with O^{2-} or HO^-producing H_2O. In addition, given that similar reactions in both dry air and humid air and faster aging process occur in humid air than dry air, the kinetics of the overall aging process were most likely controlled by the oxidation reaction of Ag^0.

Furthermore, the Pseudo reaction model with the oxidation reaction of Ag^0 from dry air and humid air aging processes is capable to describe the kinetics of deactivation on Ag^0Z. The results of iodine loading capacity and model fitting reveal that the Ag^0Z lost a significant iodine capacity when being exposed to dry air and humid air. While the kinetics of the aged Ag^0Z in dry air and humid air were suggested in this study, future work should be involved not only in further understanding of the aging processes in gas mixture of dry air and humid air, but in ascertaining alternative adsorbents which are tolerant to dry air and humid air off-gas streams.

Acknowledgement

This research was performed through funding received from the U.S. Department of Energy (DOE), Nuclear Energy University Program (NEUP) (Grant No. DE-NE0008536).

Literature Cited

1. Haefner DR; Tranter TJ. Methods of gas phase capture of iodine from fuel reprocessing off-gas: A literature survey. Technical Report No. INL/EXT-07-12299. Idaho National Laboratory, Idaho Falls, ID, 2007. 2. Jubin

RT, DelCul GD, Patton BD, Owens RS, Ramey DW, Spencer BB. Advanced fuel cycle initiative coupled end-to-end research, development, and demonstration project: integrated off-gas treatment system design and initial performance-9226, *Paper Presented at WM2009 Conference*, *Phoenix*, AZ, 2009. 3. Scheele, R. D. et al., Preliminary evaluation of spent silver mordenite disposal forms resulting from gaseous radioiodine control at Hanford's Waste Treatment Plant. Technical Report No. PNWD-3225. Battelle-Pacific Northwest Division, Richland, WA, 2002. 4. Chapman KW, Chupas PJ, Nenoff TM. Radioactive iodine capture in silver-containing mordenites through nanoscale silver iodide formation.*J Am Chem Soc.* 2010;132(26):8897-8899. 5. Jubin RT, Ramey DW, Spencer BB, Anderson KK, Robinson SM. Impact of pretreatment and aging on the iodine capture performance of silver-exchanged mordenite - 12314. In: *Paper Presented at Waste Management 2012 Conference*, *Phoenix*, *AZ*, 2012. 6. Patton KK, Bruffey SH, Jubin RT, Walker Jr JF et al., Effects of extended in-process aging of silver-exchanged mordenite on iodine capture performance, *Paper Presented at 33rd Nuclear Air Cleaning Conference*, *St. Louis*, *MO*, 2014. 7. Bruffey SH, Jubin RT, Initial evaluation of effects of NOx on iodine and methyl iodide loading of AgZ and Aerogels. Technical Report No. ORNL/SPR-2015/125. Oak Ridge National Laboratory, Oak Ridge, TN, 2015. 8. Bruffey SH, Patton KK, Walker Jr JF, Jubin RT. Complete NO and NO_2 aging study for AgZ. Technical Report No. ORNL/SPR-2015/128. Oak Ridge National Laboratory, Oak Ridge, TN, 2015. 9. Nan Y, Liu J, Tang S, Lin R, Tavlarides LL. Silver-exchanged mordenite for capture of water vapor in off-gas streams: A study of adsorption kinetics. *Industrial & Engineering Chemistry Research.* 2018;57(3):1048-1058.

10. Nan Y. Choi S, Ladshaw AP, Yiacoumi S, Tsouris C, Tavlarides LL. Determination of mechanisms and kinetics of Ag^0Z and Ag^0-Aerogel aging in nuclear off-gases, In: *Transactions of the American Nuclear Society , Vol. 118 ,Philadelphia , PA* , 2018

11. Nan Y, Tavlarides LL. Adsorption of iodine on hydrogen-reduced silver-exchanged mordenite: Experiments and modeling. *AIChE Journal* . 2017;63(3):1024-1035.

12. Shimizu K, Sugino K, Kato K, Yokota S, Okumura K, Satsuma A. Formation and redispersion of silver clusters in Ag-MFI zeolite as investigated by time-resolved QXAFS and UV-Vis. *The Journal of Physical Chemistry C* . 2007;111(4):1683-1688.

13. Abney CW, Nan Y, Tavlarides LL. X-ray absorption spectroscopy investigation of iodine capture by silver-exchanged mordenite.*Industrial & Engineering Chemistry Research* . 2017;56(16):4837-4846.

14. Zhao HY, Nenoff TM, Jennings G, Chupas PJ, Chapman KW. Determining quantitative kinetics and the structural mechanism for particle growth in porous templates. *The Journal of Physical Chemistry Letter* . 2011;2(21):2742-2746.

15. Aspromonte SG, Mizrahi MD, Schneeberger FA, Lopez JM, Boix AV. Study of the nature and location of silver in Ag-exchanged mordenite catalysts. Characterization by spectroscopic techniques. *The Journal of Physical Chemistry C* . 2013;117(48):25433-25442.

16. Beyer H, Jacobs PA, Uytterhoeven JB. Redox behaviour of transition metal ions in zeolites. Part 2.-Kinetic study of the reduction and reoxidation of silver-Y zeolites. *Journal of the Chemical Society, Faraday Transactions 1: Physical Chemistry in Condensed Phases* . 1976;72:674-685.

17. Lagergren S. Zur theorie der sogenannten adsorption geloster stoffe,*Kungliga Svenska Vetenskapsakademiens . Handlingar* . 1898;24(4):1-39.

18. Bhattacharya AK, Venkobachar C. Removal of cadmium (II) by low cost adsorbents, *Journal of Environmental Engineering* . 1984;110(1):110-122.

19. Ho YS, Mckay G. A comparison of chemisorption kinetic models applied to pollutant removal on various sorbents, *Process Safety and Environmental Protection* . 1998;76B:332-340.

20. Ho YS, Mckay G. Kinetic models for the sorption of dye from aqueous solution by wood, *Process Safety and Environmental Protection* . 1998;76B:183-191.

21. Ho YS, Mckay G. Sorption of dye from aqueous solution by peat, *Chemical Engineering Journal* . 1998;70:115-124.

22. Ho YS, Mckay G. The kinetics of sorption of basic dyes from aqueous solution by sphagnum moss peat, *The Canadian Journal of Chemical Engineering* . 1998;76:822-827.